Title	Cell shortening and calcium dynamics in epicardial and encocardial myocytes from the left ventricle of the Goto-Kalizaki type 2 diabetic rats
Type	Article
URL	https://clok.uclan.ac.uk/id/eprint/21418/
DOI	https://doi.org/10.1113/EP086542
Date	2018
Citation	Smail, Manal, Al Kury, Lina, Qureshi, Muhammad Anwar, Shmygol, Anatoliy, Oz, Murat, Singh, Jaipaul and Howarth, Frank Christopher (2018) Cell shortening and calcium dynamics in epicardial and encocardial myocytes from the left ventricle of the Goto-Kalizaki type 2 diabetic rats. Experimental Physiology. ISSN 0958-0670
Creators	Smail, Manal, Al Kury, Lina, Qureshi, Muhammad Anwar, Shmygol, Anatoliy, Oz, Murat, Singh, Jaipaul and Howarth, Frank Christopher

Title: Cell shortening and calcium dynamics in epicardial and endocardial myocytes from the left ventricle of the Goto-Kakizaki type 2 diabetic rats.

Authors:

Manal Smail – Department of Physiology, College of Medicine & Health Sciences, Al Ain, UAE University, UAE

Lina Al Kury – College of Natural and Health Sciences, Zayed University, Abu Dhabi, UAE

Muhammad Anwar Qureshi - Department of Physiology, College of Medicine & Health Sciences, Al Ain, UAE University, UAE

Anatoliy Shmygol - Department of Physiology, College of Medicine & Health Sciences, Al Ain, UAE University, UAE

Murat Oz - Department of Basic Medical Sciences, College of Medicine, Qatar University, Doha, Qatar.

Jaipaul Singh - School of Forensic & Applied Sciences, University of Central Lancashire, Preston, UK

Frank Christopher Howarth - Department of Physiology, College of Medicine & Health Sciences, Al Ain, UAE University, UAE

Running title: Regional effects of diabetes on rat ventricular myocytes

New Findings

- What is the central question of this study?

  Hemodynamic dysfunction has been widely reported in the diabetic heart. Our aim was to investigate shortening and Ca^{2+} transport in ventricular myocytes from epicardial (EPI) and endocardial (ENDO) regions of the heart in the type 2 diabetic Goto-Kakizaki (GK) rat.

- What is the main finding and its importance?

  EPI and ENDO myocytes from the GK rat displayed similar levels of hypertrophy. Time to peak (TPK) and time to half (THALF) relaxation were prolonged in EPI and ENDO myocytes, TPK Ca^{2+} transient was prolonged and THALF decay of the Ca^{2+} transient was shortened in ENDO myocytes from GK rat. Amplitude of shortening and Ca^{2+} transient and sarcoplasmic reticulum Ca^{2+} were unaltered in EPI and ENDO myocytes from GK rats compared to controls. Regional differences in shortening and Ca^{2+} transport have been demonstrated in the type 2 diabetic GK rat.

Abstract

Diabetic cardiomyopathy is considered as one of the major diabetes-associated complications and the pathogenesis of cardiac dysfunction is not well understood. The electromechanical properties of cardiac myocytes vary across the walls of the chambers The aim of this study was to investigate shortening and Ca^{2+} transport in epicardial (EPI) and endocardial (ENDO) left ventricular myocytes in the Goto-Kakizaki (GK) type 2 diabetic rat heart. Shortening and intracellular Ca^{2+} transients were measured by video edge detection and fluorescence photometry. Myocyte surface area was increased in EPI-GK and ENDO-GK compared to EPI-CON and ENDO-CON myocytes. Time to peak (TPK) shortening was prolonged in EPI-GK compared to EPI-CON and in ENDO-CON compared to EPI-CON myocytes. Time to half (THALF) relaxation of shortening was prolonged in EPI-GK compared to EPI-CON myocytes. TPK Ca^{2+} transient was prolonged in EPI-GK compared to EPI-CON myocytes. THALF decay of the Ca^{2+} transient was prolonged in EPI-CON compared to EPI-GK and in EPI-CON compared to ENDO-CON myocytes. Amplitude of shortening and the Ca^{2+} transient were unaltered in EPI-GK and ENDO-GK compared to their respective controls. Sarcoplasmic reticulum Ca^{2+} and myofilament sensitivity to Ca^{2+} were unaltered in EPI-GK and ENDO-GK compared to their respective controls. Regional differences in Ca^{2+} signaling in healthy and diabetic myocytes may account for variation in the dynamics of myocyte shortening. Further studies will be required to clarify the mechanisms underlying regional differences in the time course of shortening and the Ca^{2+} transient in EPI and ENDO myocytes from diabetic and control hearts.

Introduction

The electrical and mechanical properties of cardiac myocytes vary across the walls of the heart. The characteristic shape of the action potential changes significantly across the myocardial wall from the epicardial (EPI), midmyocardial (MID) to endocardial (ENDO) regions which can be attributed to the differential expression of ion channels. Changes in repolarizing ionic currents such as reduction in transient outward (I_{to}) and delayed rectifier (I_K) and increase in the inward rectifier (I_{K1}) in ENDO compared to EPI rat myocytes have been previously reported (Shimoni *et al.* 1995;Bryant *et al.* 1999;Volk *et al.* 1999;Yao *et al.* 1999;Wang *et al.* 2010). Mathematical modeling suggests that a smaller density and slower reactivation kinetics of I_{to} in ENDO myocytes may account for the longer action potential duration (Pandit *et al.* 2001).

In terms of ventricular myocyte size, White *et al* (1988) reported that the cross-sectional area of ENDO myocytes is greater than that of EPI myocytes and exercise training increased the size of myocytes in EPI but not ENDO regions in rat heart (White *et al.* 1988). However, a study carried by Natali *et al* (2002) demonstrated that length, width, depth, length to width ratio, volume and amplitude of shortening were similar in ENDO and EPI myocytes (Natali *et al.* 2002).

The ultrastructure of the heart may alter under several pathological conditions. For example, 14 weeks of hypertension caused an increase in left ventricular weight and wall thickness. Hypertrophy of myocytes was 76% greater in the EPI compared to ENDO region. *In vivo* echocardiography has confirmed that sub-endocardial layers contract more and faster than EPI layers of rat ventricular myocardium (Ait *et al.* 2009). In spontaneously hypertensive rats, McCrossan *et al* (2004) showed that the effect of hypertension on the morphology, mechanical activity and electrical activity of left ventricle myocytes is dependent on their transmural location. EPI, MID and ENDO myocytes from left ventricle had similar volume. Cell lengths were longer in EPI and MID compared to ENDO and cell

widths were similar in EPI, MID and ENDO and length/width were larger in EPI compared to ENDO myocytes. However, myocyte amplitude, time to peak (TPK) shortening and time to half (THALF) relaxation of shortening were similar in EPI, MID and ENDO myocytes (McCrossan *et al.* 2004). Aging also seems to play a role in the variability of results. Decay time of the Ca^{2+} transient and the time required for 50% length relaxation increased with age but not uniformly across the EPI, MID and ENDO rat ventricular myocytes (Haynes *et al.* 2014).

During the process of excitation-contraction coupling, membrane depolarization opens L-type Ca^{2+} channels. A small amount of Ca^{2+} entering via L-type Ca^{2+} channels triggers a large release of Ca^{2+} from the sarcoplasmic reticulum (SR). The rise in intracellular Ca^{2+} (Ca^{2+} transient), initiates and regulates cardiac muscle contraction. Several studies have shown that L-type Ca^{2+} channels are similar in rat ventricular myocytes from ENDO compared to EPI regions (Bryant *et al.* 1999; Volk & Ehmke, 2002; Smail *et al.* 2016). However, results on regional differences in intracellular Ca^{2+} transport in rat ventricular myocytes vary. Fowler *et al* (2005) reported larger amplitude of Ca^{2+} transient, prolonged time to peak of Ca^{2+} transient and larger amplitude of caffeine-evoked Ca^{2+} transient in rat ENDO compared to EPI ventricular myocytes (Fowler *et al.* 2005). Natali *et al* (2002) reported similar amplitude of Ca^{2+} transients in EPI and ENDO myocytes and McCrossan *et al* (2004) reported similar amplitudes of Ca^{2+} transient in EPI, MID and ENDO myocytes.

Diabetic cardiomyopathy is considered one of the major diabetes-associated complications that is reported in human patients with type 2 diabetes mellitus. This condition is characterized by a change in the structure and function of the heart, in other words, a change in electrical and mechanical performance of the heart that is independent of coronary artery disease (Sheikh *et al.* 2012). A variety of diastolic and systolic dysfunctions have been reported in type 2 diabetic patients and the severity of abnormalities depends on the patients' age and the duration of diabetes (Yasuda *et al.* 1992;Di Bonito *et al.* 1996;Chareonthaitawee *et al.* 2007). In addition to increased risk of heart attack and

stroke, cardiac electrical conduction abnormalities are also frequently observed in diabetic patients (Ewing *et al.* 1991; Lindstrom *et al.* 1992).

Alterations in Ca^{2+} regulatory mechanisms are a hallmark of cardiomyopathy and heart failure in human patients (Morgan *et al.* 1990; Sheikh *et al.* 2012). Cardiac cell contractility is controlled by intracellular Ca^{2+} cycling which is initiated by a small Ca^{2+} influx across the cell membrane via channels called L-type Ca^{2+} channels. The activation of these channels stimulates a further and larger release of Ca^{2+} from intracellular stores (sarcoplasmic reticulum) in a process called Ca^{2+}-induced Ca^{2+} release. Relaxation occurs as a result of Ca^{2+} removal from the cytoplasm into the intracellular stores and efflux cross the cell membrane, predominantly via the Na^+/Ca^{2+} exchange (Bers, 1991).

Studies in animal models have shown that diabetes results in abnormal Ca^{2+} homeostasis and alteration in ventricular excitation-contraction coupling (Morgan *et al.* 1990; Chattou *et al.* 1999; Lebeche *et al.* 2008; Howarth *et al.* 2011; Sheikh *et al.* 2012). Cardiac myocytes from diabetic heart have been shown to display reduced Ca^{2+} uptake into intracellular stores (Netticadan *et al.* 2001) and impaired Na^+/Ca^{2+} exchange function (Hattori *et al.* 2000), which partly underlies the mechanical defects observed in experimental models of diabetes. For example, Howarth *et al.* (2011) reported decreased L-type Ca^{2+} channel activity in type 2 diabetic hearts. Furthermore, Sheikh *et al* (2012) have shown that diabetes caused a significant alteration in sarcoplasmic reticulum Ca^{2+} ATPase (SERCA) and $Na^{+/}Ca^{2+}$ exchange activity.

Previous studies have demonstrated a variety of contractile dysfunctions in GK rat heart, including decreased heart rate, decreased ejection fraction and prolonged time course of shortening and/or relaxation in ventricular myocytes (Iltis *et al.* 2005; Howarth *et al.* 2007; Howarth & Qureshi, 2008). In type 2 diabetic GK rats, Salem *et al* (2012) reported changes in expression of genes encoding various excitation-contraction coupling proteins that are associated with disturbances in myocyte shortening and intracellular Ca^{2+} transport. D'Souza *et al* (2014) reported that chronic mild

hyperglycemia can produce molecular and structural correlates of hypertrophic myopathy in spontaneously type 2 diabetic rats. Recently published data have shown prolonged TPK shortening in ENDO and EPI myocytes from STZ-treated rats. THALF relaxation of shortening, TPK Ca^{2+} transient and THALF decay of Ca^{2+} transient were prolonged in ENDO myocytes from STZ-treated rats compared to ENDO controls. SR fractional release was also reduced in EPI myocytes in diabetic rat compared to controls (Smail *et al.* 2016).

Despite the available data, very little is known about the regional effects of diabetes mellitus on Ca^{2+} signaling in the ventricular myocardium. Therefore, the aim of this project was to investigate the regional effects of diabetes mellitus on shortening and Ca^{2+} transport in epicardial (EPI) and endocardial (ENDO) myocytes from the left ventricles of GK type 2 diabetic rats.

Methods

Ethical Approval

Male GK rats (aged 3 months) were obtained from Taconic, Germantown, NY, USA. Male age-matched Control Wistar rats were bred in our Animal House Facility. Rats were kept in cages, under a 12 h-12 h light-dark cycle, and had free access to food and tap water.   Room temperature was kept between 21 and 25 °C. Experiments commenced when the animals were 12 months of age. Ethical approval for this project was obtained from the UAE University Animal Research Ethics Committee. The Ethics Committee reference number was A11-15 dated 2-3-2015. The authors understand and complied with all ethical principles that the journal upholds.

Experimental model: Experiments were performed in male GK rat, a well characterized experimental model of type 2 diabetes mellitus (Kristiansen *et al.* 2004; Liepinsh *et al.* 2009; Howarth *et al.* 2007; Howarth *et al.* 2008). Fasting blood glucose and glucose tolerance measurements were taken by previously described methods (D'Souza *et al.* 2014). In brief, after an overnight fast, animals aged 12 months, were injected intraperitoneally (ip) with 2 g glucose/kg body weight. Glucose was dissolved in water and animals were injected with 1.15-1.20 ml of the resulting glucose solution in order to achieve the desired dose of 2 g glucose/kg body weight. Small drops of blood were collected from a nick applied to the tip of the tail. Blood glucose was measured at time zero (fasting blood glucose), 30, 60, 120 and 180 min after glucose injection. Bodyweight, non-fasting blood glucose and heart weight were measured prior to experiments. Experiments were performed in EPI and ENDO myocytes from left ventricle of GK and age-matched Wistar control rats from 12 months of age.

Isolation of ventricular myocytes: Ventricular myocytes were isolated according to modifications of previously described techniques (Smail *et al.* 2016). In brief, animals were euthanized using a guillotine. This approach was used to minimize the risk of damage to the heart and associated blood vessels. Hearts were removed rapidly and mounted for retrograde perfusion on a Langendorff system. Hearts were perfused at a constant flow rate of 8 ml.g heart^{-1}.min^{-1} and at 36-37 ºC with cell isolation solution containing in mmol/l: 130.0 NaCl, 5.4 KCl, 1.4 MgCl$_2$, 0.75 CaCl$_2$, 0.4 NaH$_2$PO$_4$, 5.0 HEPES, 10.0 glucose, 20.0 taurine and 10.0 creatine (pH 7.3). When heart contraction had stabilized, perfusion was switched for 4 min to Ca^{2+}-free cell isolation solution containing 0.1 mmol/l EGTA, and then for 6 min to cell isolation solution containing 0.05 mmol/l Ca^{2+}, 0.60 mg/ml type 1 collagenase (Worthington Biochemical Corp, Lakewood, NJ, USA) and 0.075 mg/ml type XIV protease (Sigma,

Taufkirchen, Germany). Left ventricle tissue was excised from the heart, a section of tissue was carefully dissected from ENDO and EPI regions, minced and gently shaken in collagenase-containing isolation solution supplemented with 1 % BSA. Cells were filtered from this solution at 4 min intervals and re-suspended in cell isolation solution containing 0.75 mmol/l Ca^{2+}.

Measurement of ventricular myocyte shortening: Ventricular myocytes were isolated and shortening measured according to modifications of previously described techniques (Smail *et al.* 2016). In brief cells were superfused (3-5 ml/min) with normal Tyrode containing the following in mmol/l: 140.0 NaCl, 5.0 KCl, 1.0 $MgCl_2$, 10.0 glucose, 5.0 HEPES, 1.8 $CaCl_2$ (pH 7.4). Unloaded EPI and ENDO myocyte shortening were recorded using a video edge detection system (VED-114, Crystal Biotech, Northborough, MA, USA). Resting cell length, TPK shortening, THALF relaxation and amplitude of shortening (expressed as a % of resting cell length) were measured in electrically stimulated (1 Hz) myocytes maintained at 35-36 °C. Data was acquired and analyzed with Signal Averager software v 6.37 (Cambridge Electronic Design, Cambridge, UK).

Measurement of intracellular Ca^{2+}: Myocyte fura-2 ratio (intracellular Ca^{2+}) was measured in fura-2 AM loaded myocytes according to previously described techniques (Smail *et al.* 2016). In brief, cells were alternately illuminated by 340 nm and 380 nm light using a monochromator (Cairn Research, Faversham, UK) which changed the excitation light every 2 ms. The resulting fluorescence emitted at 510 nm was recorded by a photomultiplier tube and the ratio of the emitted fluorescence at the two excitation wavelengths (340/380 ratio) provided an index of intracellular Ca^{2+} concentration. Resting fura-2 ratio, TPK Ca^{2+} transient, THALF decay of the Ca^{2+} transient and the amplitude of the Ca^{2+} transient were measured in electrically stimulated (1 Hz) myocytes maintained at 35-36 °C. Data

were acquired and analyzed with Signal Averager software v 6.37 (Cambridge Electronic Design, Cambridge, UK).

Measurement of sarcoplasmic reticulum Ca^{2+} transport: SR Ca^{2+} was assessed using previously described techniques (Smail *et al.* 2016). The protocol employed in this study is illustrated in Figure 5a. In brief, after establishing steady state Ca^{2+} transients in electrically stimulated (1 Hz) myocytes maintained at 35-36 °C and loaded with fura-2 AM, stimulation was paused for a period of 5 sec. Caffeine (20 mM) was then applied for 10 sec using a solution switching device customized for rapid solution exchange (Levi *et al.* 1996). Electrical stimulation was then resumed and the Ca^{2+} transients allowed to recover to steady state. Fractional release of SR Ca^{2+} was calculated by comparing the amplitude of the electrically-evoked steady state Ca^{2+} transients with that of the caffeine-evoked Ca^{2+} transient.

Measurement of myofilament sensitivity to Ca^{2+}: In some cells shortening and fura-2 ratio were recorded simultaneously (Hamouda *et al.* 2015). Myofilament sensitivity to Ca^{2+} was assessed from phase-plane diagrams of fura-2 ratio versus cell length by measuring the gradient of the fura-2 - cell length trajectory during the late relaxation of the twitch contraction. The position of the trajectory reflects the relative myofilament response to Ca^{2+} and hence, can be used as a measure of myofilament sensitivity to Ca^{2+} (Spurgeon *et al.* 1992).

Statistics: The results were expressed as the mean ± Standard Deviation (SD) of 'n' observations. Statistical comparisons were performed using either Independent samples t-test or one-way ANOVA

followed by Bonferroni corrected t-tests for multiple comparisons, as appropriate. p < 0.05 was considered significant.

Results

General characteristics: The general characteristics of GK rats compared to age-matched controls are shown in Table 1. GK rats displayed significantly ($p<0.01$) increased heart weight and heart weight / body weight ratio and increased non-fasting blood glucose compared to controls.

Table 1 – General characteristics of the Goto-Kakizaki rat

	Control	**Goto-Kakizaki**
Body weight (g)	457.75±50.24(12)	432.70±25.64(10)
Heart weight (g)	1.39±0.18(12)	1.72±0.22(10)**
Heart weight / Body weight (mg/g)	3.01±0.39(12)	4.00±0.65(10)**
Blood glucose (mg/dl)	86.08±9.05(12)	182.70±31.90(10)**

Data are mean ± SD, number in parenthesis is the number of animals.

** $p<0.01$

Glucose clearance capacity was significantly reduced in GK animals as blood glucose levels following glucose tolerance tests were higher at all the time points measured ($p<0.01$) and did not return to baseline level within 3 h (Fig. 1).

Ventricular myocyte shortening: Length, width and surface area of myocytes are shown in Fig. 2A-C. The length, width and calculated surface area were significantly (p<0.05) increased, and to similar extents, in EPI and ENDO myocytes from GK rats compared to controls (Fig. 2A-C). Typical records of shortening in EPI-CON and EPI-GK myocytes are shown in Fig. 3A. TPK shortening was significantly prolonged in EPI-GK (91±20 ms) compared to EPI-CON (78±17 ms) myocytes but was not altered in ENDO-GK compared to ENDO-CON myocytes (Fig 3B). Regionally, in control myocytes there was also a significant prolongation in ENDO-CON (88±20 ms) compared to EPI-CON (78±17 ms) myocytes (Fig. 3B). When TPK shortening was normalized to AMP shortening there were no significant differences (p>0.05) between EPI-CON (17.45±6.69 ms/AMP), EPI-GK (19.22±8.82 ms/AMP), ENDO-CON (18.96±7.08 ms/AMP) and ENDO-GK (20.47±7.71 ms/AMP). THALF recovery of shortening was also prolonged in EPI-GK (60±27 ms) compared to EPI-CON (47±18 ms) myocytes (Fig. 3C). The amplitude of shortening was not significantly (p>0.05) altered in EPI-GK or ENDO-GK compared to respective controls (Fig. 3D).

Intracellular Ca^{2+}: Typical records of Ca^{2+} transients in EPI-CON and EPI-GK myocytes are shown in Fig. 4A. Resting fura-2 ratio was not significantly (p>0.05) altered in EPI-GK compared to EPI-CON or ENDO-GK compared to ENDO-CON myocytes (Fig. 4B). TPK Ca^{2+} transient was significantly (p<0.05) prolonged in EPI-GK (55±13 ms) compared to EPI-CON (50±9 ms) myocytes (Fig. 4C). When the TPK Ca^{2+} transient was normalized to AMP Ca^{2+} transient there were no significant differences (p>0.05) between EPI-CON (339±165 ms/RU), EPI-GK (334±240 ms/RU), ENDO-CON (347±200 ms/RU) and ENDO-GK (346±215 ms/RU). THALF decay of the Ca^{2+} transient was significantly (p<0.05) prolonged in EPI-CON (149±52 ms) compared to EPI-GK (121±6 ms) myocytes and was also significantly prolonged in EPI-CON (149±6 ms) compared to ENDO-

CON (123±40 ms) myocytes (Fig. 4D). The amplitude of the Ca^{2+} transient was not significantly (p>0.05) altered in EPI-GK or ENDO-GK compared to respective controls (Fig. 4E).

Sarcoplasmic reticulum Ca^{2+}: A typical record showing the protocol employed in these experiments is shown in Fig. 5A. The amplitude of caffeine-evoked (Fig. 5B) Ca^{2+} transients were not significantly (p>0.05) altered in EPI-GK or ENDO-GK compared to respective controls. Area under the caffeine-evoked Ca^{2+} transient curve (Fig. 5C) and fractional release of Ca^{2+} (calculated by comparing the amplitude of the electrically-evoked steady state Ca^{2+} transients with that of the caffeine-evoked Ca^{2+} transient) (Fig. 5D) were not significantly (p>0.05) altered in EPI-GK and ENDO-GK compared to respective controls.

Myofilament sensitivity to Ca^{2+}: Typical recordings of myocyte shortening and Ca^{2+} transient and a phase-plane diagram of Fura-2 ratio versus cell length are shown in Fig. 6A (left and right panels). Myofilament sensitivity to Ca^{2+} was assessed by measuring the gradient of the Fura-2 – cell length trajectory during late relaxation of the twitch contraction. The position of the trajectory reflects the relative myofilament response to Ca^{2+} and hence, can be used as a measure of myofilament sensitivity to Ca^{2+} (Spurgeon *et al.* 1992). The gradient of the trajectory during the period 500-800 ms was not significantly (p>0.05) altered in EPI-GK and ENDO-GK compared to respective controls (Fig. 6B).

Discussion

In this study, experiments were performed in EPI and ENDO myocytes from left ventricle of GK and age-matched Wistar control rats from 12 months of age. The major findings of this study were: (i) Myocyte length, width and surface area were increased to similar extents in EPI-GK compared to

EPI-CON and in ENDO-GK compared to ENDO-CON myocytes, (ii) Kinetic properties of shortening and Ca transients were not different in EPI-GK compared to EPI-CON and in ENDO-CON compared to EPI-CON myocytes, (iii) Amplitudes of cell shortening and Ca^{2+} transients were similar in EPI-GK compared to EPI-CON and in ENDO-CON compared to EPI-CON myocytes; (iv) Area under the curve of the caffeine-evoked Ca^{2+} transient and SR fractional release of Ca^{2+} were unaltered in EPI and ENDO from GK and CON myocytes and (v) Myofilament sensitivity to Ca^{2+} was unaltered in EPI and ENDO from GK and CON myocytes.

The results of this work show that length, width and calculated surface area were increased in EPI-GK compared to EPI-CON and in ENDO-GK compared to ENDO-CON myocytes. These findings are consistent with the results of a study conducted by D'Souza *et al.* (2014) who showed that chronic mild hyperglycemia causes structural remodeling of left ventricle and cardiomyocyte hypertrophy in type 2 diabetic GK rats. Differences have also been reported in other regional cell measurements. For example, White *et al* (1988) reported that the cross-sectional area is greater in ENDO compared to EPI myocytes, whilst De Clerck *et al.* (1984) reported no significant difference between resting cell dimensions and sarcomere length in EPI and ENDO. The heart weight to body weight ratio was significantly increased in GK rats compared with control rats, a finding that is consistent with previous studies (Salem *et al.* 2013; El Omar *et al.* 2004; D'Souza *et al.* 2014). Absolute values of the TPK shortening was prolonged in EPI-GK compared to EPI-CON and in ENDO-CON compared to EPI-CON myocytes. Our recent study which employed the streptozotocin (STZ) model of diabetes reported prolonged TPK shortening in EPI-STZ and also in ENDO-STZ compared to respective controls (Smail *et al.* 2016). In the present study however, there was no statistically significant difference between GK and control groups when TPK shortening was normalized to peak shortening. Interestingly, in the type1 STZ diabetic model there was no change in EPI-STZ however, THALF relaxation was prolonged in ENDO-STZ compared to respective controls (Smail *et al.* 2016). The amplitude of shortening was similar in EPI and ENDO myocytes from GK rats and controls, a finding

that is consistent with previous regional myocyte results in myocytes from the STZ rat (Smail *et al.* 2016) and generally in a single population of ventricular myocytes in the GK rat (Salem *et al.* 2012; Howarth *et al.* 2007). The lack of changes in the parameters of cell shortening between the GK and control groups are in stark contrast to the results obtained in multicellular preparations of trabecular muscle from STZ diabetic animals (Zhang *et al.* 2008). The authors of that study observed a substantial reduction in peak isometric force, decreased rate of force development and decreased rate of relaxation. While we cannot rule out potential differences between the GK and STZ models of diabetes, most likely reason for the discrepancies lies in the differences between experimental approaches in these two studies, namely single cell unloaded shortening vs isometric contraction of multicellular tissue.

Indeed, previous studies have variously demonstrated increased collagen deposition and increased ventricular stiffness in different experimental models of type 2 diabetes, which in turn were associated with altered kinetics of myocardial contraction (Patel *et al.* 2009; Rickman *et al.* 2010).

Resting values of fura-2 ratio were similar in EPI-GK and ENDO-GK compared to respective controls suggesting that resting Ca^{2+} concentration was unaltered by diabetes. This was a similar result to that previously reported in EPI and ENDO myocytes and in trabecular preparations from the STZ rat (Smail *et al.* 2016; Zhang *et al.* 2008). TPK Ca^{2+} transient was similar in control EPI and ENDO myocytes. However, the TPK Ca^{2+} transient was prolonged in EPI-GK compared to EPI-CON myocytes. In the STZ rat there were no changes in EPI-STZ compared to EPI-CON however, ENDO-STZ was prolonged compared to ENDO-CON myocytes (Smail *et al.* 2016). Previous studies have also reported prolonged TPK Ca^{2+} transient in a single population of myocytes from GK heart (Gaber *et al.* 2014). This might be explained by altered flux of Ca^{2+} through L-type Ca^{2+} channel or release of Ca^{2+} from the SR. THALF decay of the Ca^{2+} transient was also prolonged in EPI-CON compared to EPI-GK and in EPI-CON compared to ENDO-CON myocytes. The decay of Ca^{2+} transient is partly dependent on efflux of Ca^{2+}, primarily on Na^+/Ca^{2+} exchange and uptake of Ca^{2+} by the SR. In the

STZ rat THALF decay of the Ca^{2+} transient was prolonged in ENDO-STZ compared to ENDO-CON and in EPI-CON compared to ENDO-CON myocytes (Smail *et al.* 2016). Consistent with the shortening results, there was no significant variation in the amplitude of Ca^{2+} transient in ENDO and EPI from control and GK ventricular myocytes. Collectively, the results of intracellular Ca^{2+} dynamics demonstrate regional differences in time course of Ca^{2+} transient in healthy ventricle, in addition to differences that can be attributed to diabetes.

SR Ca^{2+} content was similar in EPI and ENDO myocytes from GK rats and controls. This is evident from SR fractional release of Ca^{2+} and area under the curve of the caffeine stimulated Ca^{2+} transient that were unaltered in EPI and ENDO from GK and CON myocytes.

The Na^+/Ca^{2+} exchange is a major pathway for Ca^{2+} extrusion during relaxation of cardiac muscle, and therefore it is an important mediator for Ca^{2+} homeostasis (Hattori *et al.*, 2000). Therefore, it is possible that the decrease in Ca^{2+} transients observed in EPI-GK and ENDO-GK may be attributed to altered activity of Na^+/Ca^{2+} exchange during Ca^{2+} efflux. A study conducted by Sheikh *et al* (2012) demonstrated that cardiac endothelial cells from diabetic rat treated with Na^+/Ca^{2+} exchange inhibitor had a higher intracellular Ca^{2+} transient peak as compared to no inhibitor controls (Sheikh *et al.* 2012).

In view of the ability of mitochondria to accumulate large amounts of Ca^{2+}, these organelles are known to prevent and/or delay the occurrence of intracellular Ca^{2+} overload in cardiomyocytes under different pathological conditions. For example, during the development of cardiac dysfunction and intracellular Ca^{2+} overload in chronic diabetes, mitochondria are believed to continue accumulating Ca^{2+}, serving as a protective mechanism (Dhalla *et al.* 1998; Dhalla *et al.* 2012). Therefore, it is possible that altered mitochondrial uptake of Ca^{2+} during diabetes is responsible for decreased Ca^{2+} transients observed here. Although mitochondria are being established as a contributor to cellular Ca^{2+} signaling, the exact role of changes in these mechanisms in diabetic cardiomyopathy remains to

be investigated.

Myofilament sensitivity to Ca^{2+} was unaltered at this stage of diabetes. This result is consistent with an earlier study that showed no effect of type 2 diabetes on myofilament sensitivity in ventricular myocytes from young Goto-Kakizaki rat (Howarth *et al.* 2011). However, a previous study in 18 months-old, type 2 diabetic Goto-Kakizaki rats reported an increase in gradient of the fura-2-cell length trajectory, suggesting that myofilament sensitivity to Ca^{2+} may alter during the later stages of type 2 diabetes (Howarth & Qureshi, 2008).

The results of this study have demonstrated differences in the time course of shortening and Ca^{2+} transient in EPI compared to ENDO myocytes from GK compared to control rat heart. Prolonged time course of the Ca^{2+} transient may partly underlie prolonged time course of shortening in EPI myocytes from GK compared to control rat heart. Further studies will be required to clarify the mechanisms underlying the changes in the time course of shortening and the Ca^{2+} transient in EPI and ENDO myocytes from diabetic and control hearts.

Author contributions

MS was involved in analysis and critical revision; LA, AS, MO and JS were involved in conception, design and critical revision; MAQ was involved in acquisition and critical revision; FCH was involved in conception, design, interpretation of data, drafting and critical revision. All authors approved the final version of the manuscript and agree to be accountable for all aspects of the work in ensuring that questions related to the accuracy or integrity of any part of the work are appropriately investigated and resolved and that all persons designated as authors qualify for authorship, and all those who qualify for authorship are listed.

References

Ait MY, Reboul C, Andre L, Lacampagne A, & Cazorla O (2009). Late exercise training improves non-uniformity of transmural myocardial function in rats with ischaemic heart failure. *Cardiovasc Res* **81**, 555-564.

Bers DM (1991). Ca regulation in cardiac muscle. *Med Sci Sports Exerc* **23,** 1157-1162.

Bryant SM, Shipsey SJ, & Hart G (1999). Normal regional distribution of membrane current density in rat left ventricle is altered in catecholamine-induced hypertrophy. *Cardiovasc Res* **42,** 391-401.

Chareonthaitawee P, Sorajja P, Rajagopalan N, Miller TD, Hodge DO, Frye RL, & Gibbons RJ (2007). Prevalence and prognosis of left ventricular systolic dysfunction in asymptomatic diabetic patients without known coronary artery disease referred for stress single-photon emission computed tomography and assessment of left ventricular function. *Am Heart J* **154,** 567-574.

Chattou S, Diacono J, & Feuvray D (1999). Decrease in sodium-calcium exchange and calcium currents in diabetic rat ventricular myocytes. *Acta Physiol Scand* **166,** 137-144.

D'Souza A, Howarth FC, Yanni J, Dobrzynski H, Boyett MR, Adeghate E, Bidasee KR, Singh J (2014). Chronic effects of mild hyperglycaemia on left ventricle transcriptional profile and structural remodelling in the spontaneously type 2 diabetic Goto-Kakizaki rat. *Heart Fail Rev* **19,** 65-74.

Dhalla NS, Liu X, Panagia V, & Takeda N (1998). Subcellular remodeling and heart dysfunction in chronic diabetes [editorial]. *Cardiovasc Res* **40,** 239-247.

Dhalla NS, Rangi S, Zieroth S, & Xu YJ (2012). Alterations in sarcoplasmic reticulum and mitochondrial functions in diabetic cardiomyopathy. *Exp Clin Cardiol* **17,** 115-120.

Di Bonito P, Cuomo S, Moio N, Sibilio G, Sabatini D, Quattrin S, & Capaldo B (1996). Diastolic dysfunction in patients with non-insulin-dependent diabetes mellitus of short duration. *Diabet Med* **13,** 321-324.

El Omar MM, Yang ZK, Phillips AO, & Shah AM (2004). Cardiac dysfunction in the Goto-Kakizaki rat. A model of type II diabetes mellitus. *Basic Res Cardiol* **99,** 133-141.

Ewing DJ, Boland O, Neilson JM, Cho CG, & Clarke BF (1991). Autonomic neuropathy, QT interval lengthening, and unexpected deaths in male diabetic patients. *Diabetologia* **34,** 182-185.

Fowler MR, Naz JR, Graham MD, Bru-Mercier G, Harrison SM, & Orchard CH (2005). Decreased Ca2+ extrusion via Na+/Ca2+ exchange in epicardial left ventricular myocytes during compensated hypertrophy. *Am J Physiol* **288,** H2431-H2438.

Gaber EM, Jayaprakash P, Qureshi MA, Parekh K, Oz M, Adrian TE, & Howarth FC (2014). Effects of a sucrose-enriched diet on the pattern of gene expression, contraction and Ca(2+) transport in Goto-Kakizaki type 2 diabetic rat heart. *Exp Physiol* **99,** 881-893.

Hamouda NN, Sydorenko V, Qureshi MA, Alkaabi JM, Oz M, & Howarth FC (2015). Dapagliflozin reduces the amplitude of shortening and Ca(2+) transient in ventricular myocytes from streptozotocin-induced diabetic rats. *Mol Cell Biochem* **400,** 57-68.

Hattori Y, Matsuda N, Kimura J, Ishitani T, Tamada A, Gando S, Kemmotsu O, & Kanno M (2000). Diminished function and expression of the cardiac Na+-Ca2+ exchanger in diabetic rats: implication in Ca2+ overload. *J Physiol* **527** Pt 1, 85-94.

Haynes P, Nava KE, Lawson BA, Chung CS, Mitov MI, Campbell SG, Stromberg AJ, Sadayappan S, Bonnell MR, Hoopes CW, & Campbell KS (2014). Transmural heterogeneity of cellular level power output is reduced in human heart failure. *J Mol Cell Cardiol* **72:**1-8.

Howarth FC, Jacobson M, Shafiullah M, & Adeghate E (2008). Long-term effects of type 2 diabetes mellitus on heart rhythm in the Goto-Kakizaki rat. *Exp Physiol* **93,** 362-369.

Howarth FC & Qureshi MA (2008). Myofilament sensitivity to Ca2+ in ventricular myocytes from the Goto-Kakizaki diabetic rat. *Mol Cell Biochem* **315**, 69-74.

Howarth FC, Qureshi MA, Hassan Z, Al Kury LT, Isaev D, Parekh K, Yammahi SR, Oz M, Adrian TE, & Adeghate E (2011). Changing pattern of gene expression is associated with ventricular myocyte dysfunction and altered mechanisms of Ca2+ signalling in young type 2 Zucker diabetic fatty rat heart. *Exp Physiol* **96,** 325-337.

Howarth FC, Shafiullah M, & Qureshi MA (2007). Chronic effects of type 2 diabetes mellitus on cardiac muscle contraction in the Goto-Kakizaki rat. *Exp Physiol* **92,** 1029-1036.

Iltis I, Kober F, Desrois M, Dalmasso C, Lan C, Portha B, Cozzone PJ, & Bernard M (2005). Defective myocardial blood flow and altered function of the left ventricle in type 2 diabetic rats: a noninvasive in vivo study using perfusion and cine magnetic resonance imaging. *Invest Radiol* **40,** 19-26.

Kristiansen SB, Lofgren B, Stottrup NB, Khatir D, Nielsen-Kudsk JE, Nielsen TT, Botker HE, & Flyvbjerg A (2004). Ischaemic preconditioning does not protect the heart in obese and lean animal models of type 2 diabetes. *Diabetologia* **47,** 1716-1721.

Lebeche D, Davidoff AJ, & Hajjar RJ (2008). Interplay between impaired calcium regulation and insulin signaling abnormalities in diabetic cardiomyopathy. *Nat Clin Pract Cardiovasc Med* **5,** 715-724.

Levi AJ, Hancox JC, Howarth FC, Croker J, & Vinnicombe J (1996). A method for making rapid changes of superfusate whilst maintaining temperature at 37 degrees C. *Pfluügers Arch* **432,** 930-937.

Liepinsh E, Vilskersts R, Zvejniece L, Svalbe B, Skapare E, Kuka J, Cirule H, Grinberga S, Kalvinsh I, & Dambrova M (2009). Protective effects of mildronate in an experimental model of type 2 diabetes in Goto-Kakizaki rats. *Br J Pharmacol* **157,** 1549-1556.

Lindstrom T, Jorfeldt L, Tegler L, & Arnqvist HJ (1992). Hypoglycaemia and cardiac arrhythmias in patients with type 2 diabetes mellitus. *Diabet Med* **9,** 536-541.

McCrossan ZA, Billeter R, & White E (2004). Transmural changes in size, contractile and electrical properties of SHR left ventricular myocytes during compensated hypertrophy. *Cardiovasc Res* **63,** 283-292.

Morgan JP, Erny RE, Allen PD, Grossman W, & Gwathmey JK (1990). Abnormal intracellular calcium handling, a major cause of systolic and diastolic dysfunction in ventricular myocardium from patients with heart failure. *Circulation* **81,** III21-III32.

Natali AJ, Wilson LA, Peckham M, Turner DL, Harrison SM, & White E (2002). Different regional effects of voluntary exercise on the mechanical and electrical properties of rat ventricular myocytes. *J Physiol* **541,** 863-875.

Netticadan T, Temsah RM, Kent A, Elimban V, & Dhalla NS (2001). Depressed levels of Ca2+-cycling proteins may underlie sarcoplasmic reticulum dysfunction in the diabetic heart. *Diabetes* **50,** 2133-2138.

Pandit SV, Clark RB, Giles WR, & Demir SS (2001). A mathematical model of action potential heterogeneity in adult rat left ventricular myocytes. *Biophys J* **81,** 3029-3051.

Patel J, Iyer A, & Brown L (2009). Evaluation of the chronic complications of diabetes in a high fructose diet in rats. *Indian J Biochem Biophys* **46,** 66-72.

Rickman C, Iyer A, Chan V, & Brown L (2010). Green tea attenuates cardiovascular remodelling and metabolic symptoms in high carbohydrate-fed rats. *Curr Pharm Biotechnol* **11,** 881-886.

Salem KA, Adrian TE, Qureshi MA, Parekh K, Oz M, & Howarth FC (2012). Shortening and intracellular Ca2+ in ventricular myocytes and expression of genes encoding cardiac muscle proteins in early onset type 2 diabetic Goto-Kakizaki rats. *Exp Physiol* **97,** 1281-1291.

Salem KA, Qureshi MA, Sydorenko V, Parekh K, Jayaprakash P, Iqbal T, Singh J, Oz M, Adrian TE, & Howarth FC (2013). Effects of exercise training on excitation-contraction coupling and related mRNA expression in hearts of Goto-Kakizaki type 2 diabetic rats. *Mol Cell Biochem* **380,** 83-96.

Sheikh AQ, Hurley JR, Huang W, Taghian T, Kogan A, Cho H, Wang Y, & Narmoneva DA (2012). Diabetes alters intracellular calcium transients in cardiac endothelial cells. *PLoS ONE* **7,** e36840.

Shimoni Y, Severson D, & Giles W (1995). Thyroid status and diabetes modulate regional differences in potassium currents in rat ventricle. *J Physiol* **488,** 673-688.

Smail MM, Qureshi MA, Shmygol A, Oz M, Singh J, Sydorenko V, Arabi A, Howarth FC, & Al KL (2016). Regional effects of streptozotocin-induced diabetes on shortening and calcium transport in epicardial and endocardial myocytes from rat left ventricle. *Physiol Rep* **4,** e13034.

Spurgeon HA, DuBell WH, Stern MD, Sollott SJ, Ziman BD, Silverman HS, Capogrossi MC, Talo A, & Lakatta EG (1992). Cytosolic calcium and myofilaments in single rat cardiac myocytes achieve a dynamic equilibrium during twitch relaxation. *J Physiol* **447,** 83-102.

Volk T & Ehmke H (2002). Conservation of L-type Ca2+ current characteristics in endo- and epicardial myocytes from rat left ventricle with pressure-induced hypertrophy. *Pflügers Arch* **443,** 399-404.

Volk T, Nguyen TH, Schultz JH, & Ehmke H (1999). Relationship between transient outward K+ current and Ca2+ influx in rat cardiac myocytes of endo- and epicardial origin. *J Physiol* **519** Pt 3:841-50.

Wang RX, Li XR, Guo T, Sun LP, Guo SX, Yang ZY, Yang XJ, & Jiang WP (2010). Docosahexaenoic acid has influence on action potentials and transient outward potassium currents of ventricular myocytes. *Lipids Health Dis* **9:** 39. doi: 10.1186/1476-511X-9-39.

White FC, Witzel G, Breisch EA, Bloor CM, & Nimmo LE (1988). Regional capillary and myocyte distribution in normal and exercise trained male and female rat hearts. *Am J Cardiovasc Pathol* **2,** 247-253.

Yao JA, Jiang M, Fan JS, Zhou YY, & Tseng GN (1999). Heterogeneous changes in K currents in rat ventricles three days after myocardial infarction. *Cardiovasc Res* **44,** 132-145.

Yasuda I, Kawakami K, Shimada T, Tanigawa K, Murakami R, Izumi S, Morioka S, Kato Y, & Moriyama K (1992). Systolic and diastolic left ventricular dysfunction in middle-aged asymptomatic non-insulin-dependent diabetics. *J Cardiol* **22,** 427-438.

Zhang L, Cannell MB, Phillips AR, Cooper GJ, & Ward ML (2008). Altered calcium homeostasis does not explain the contractile deficit of diabetic cardiomyopathy. Diabetes 57 (8), 2158-2166.

Figure legends

Figure 1 – Glucose tolerance

Graph showing blood glucose after an overnight fast and following an intraperitoneal injection of glucose (2 g glucose / kg body weight). Data are mean ± SD, ** $p < 0.01$, n=10 hearts.
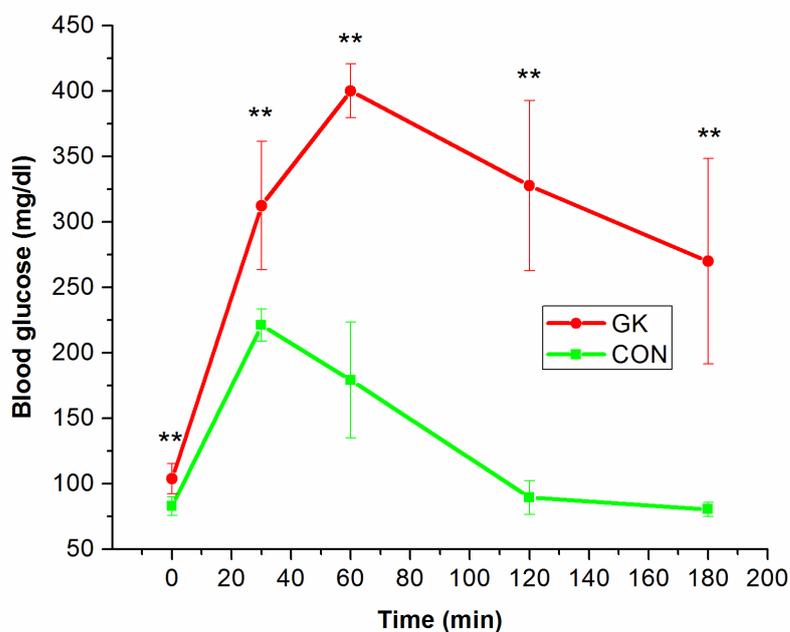

Figure 2 – Length, width and surface area of ventricular myocytes

Graphs showing the length (A), width (B), and surface area (C), of EPI and ENDO ventricular myocytes from GK and CON rats. The length and width were physically measured with a ruler and the size in microns calibrated with a standard graticule. Data are mean ± SD, n=57-88 cells from 10-

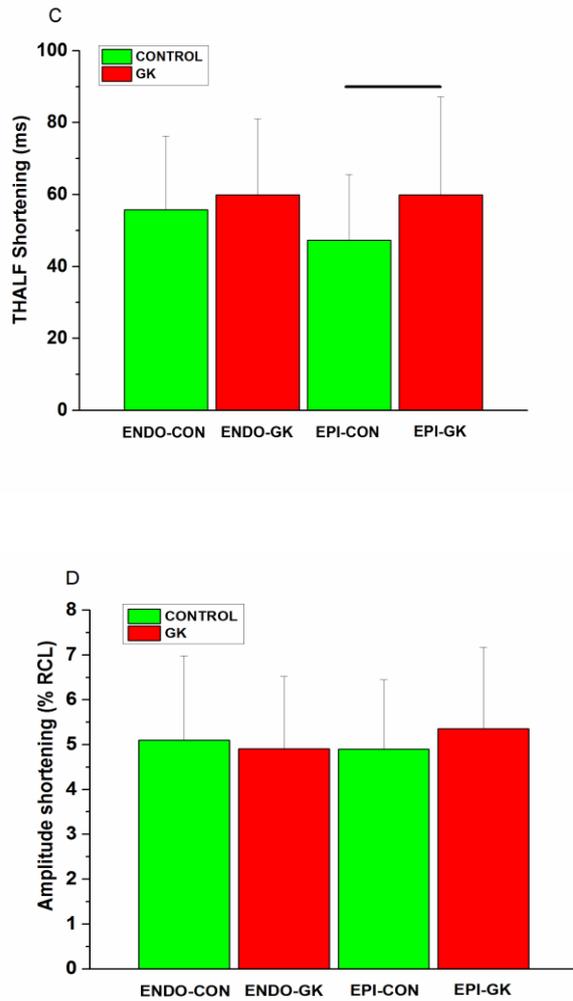12 GK and CON hearts. Horizontal lines above the bars represent significant differences at the level of p < 0.05.
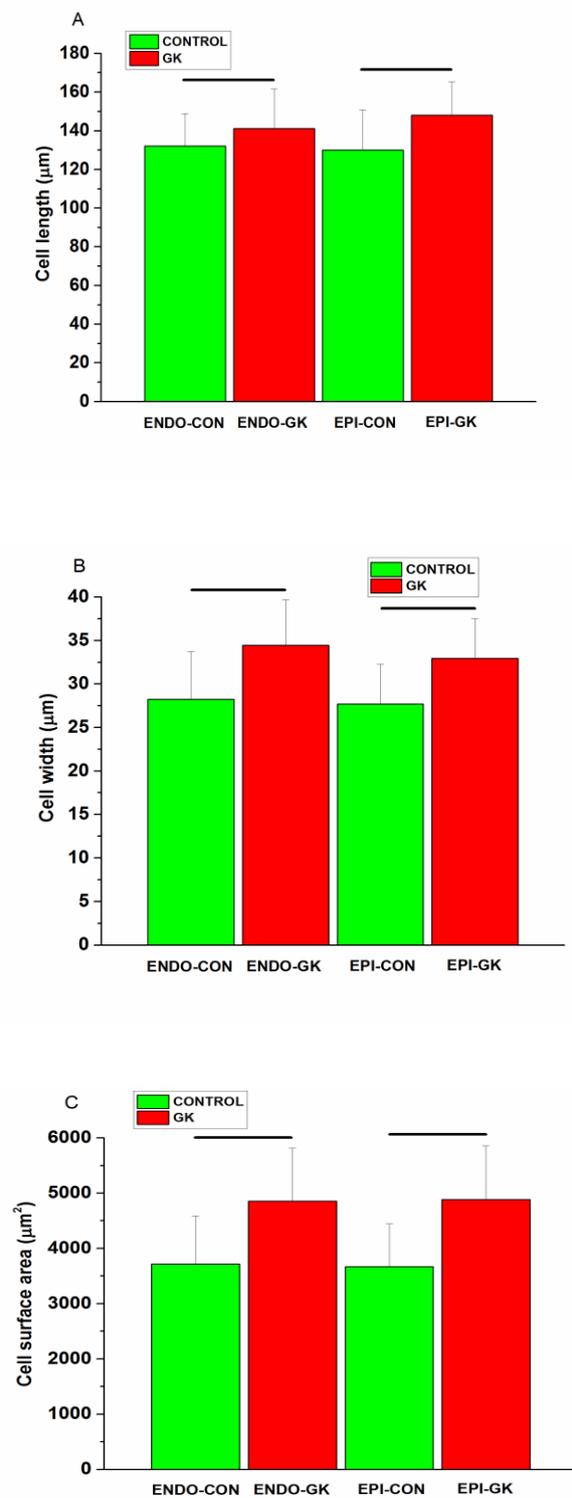
Figure 3 - Ventricular myocyte shortening

Typical records of shortening in EPI-CON and EPI-GK myocytes (A). Bar graphs showing the mean time to peak (TPK) shortening (B), time to half (THALF) relaxation of shortening (C), and amplitude of shortening (D). Data are mean ± SD, n=57-58 cells from 10-12 GK and CON hearts. Horizontal lines above the bars represent significant differences at the level of $p < 0.05$.

C

D
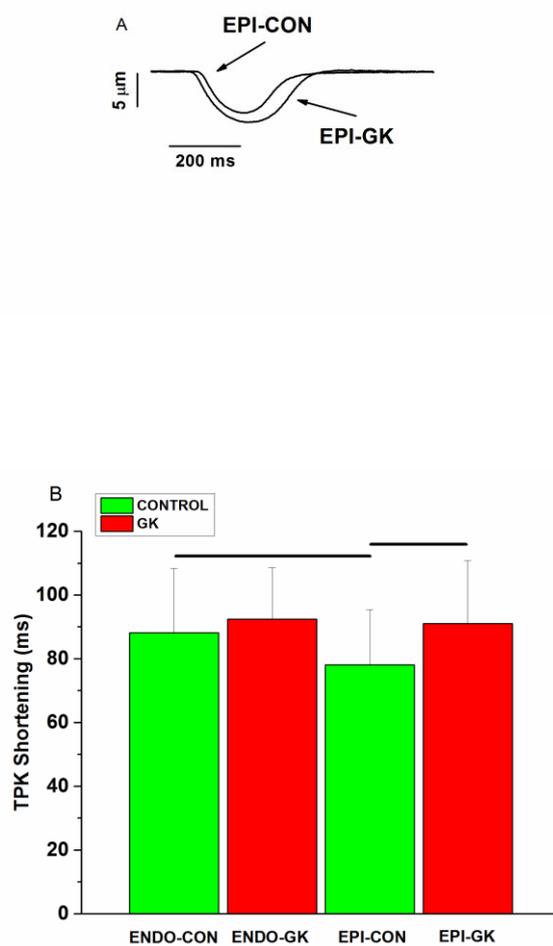
Figure 4 - Ventricular myocyte Ca^{2+} transient

Typical records of Ca^{2+} transients in EPI-CON and EPI-GK myocytes (A). Bar graphs showing the

mean resting Fura-2 ratio (B), time to peak (TPK) Ca^{2+} transient (C), time to half (THALF) decay of

the Ca^{2+} transient (D), and amplitude of the Ca^{2+} transient (E). Data are mean ± SD, n=57-86 cells

from 10-12 GK and CON hearts. Horizontal lines above the bars represent significant differences at
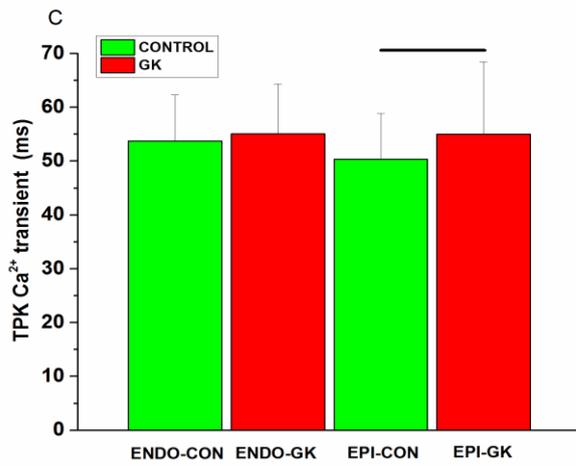
the level of $p < 0.05$.

A

EPI-GK

0.1 RU

EPI-CON

200 ms

B
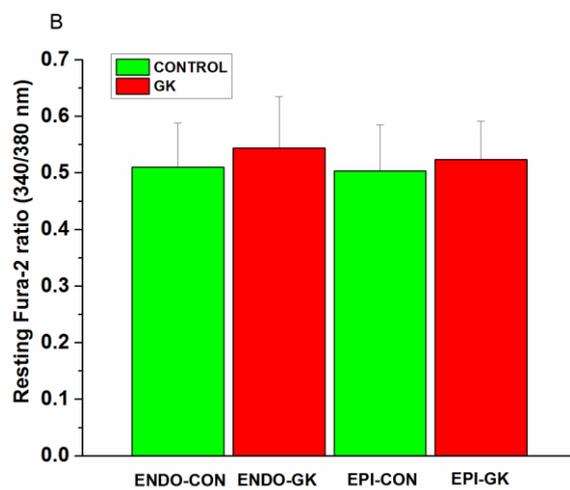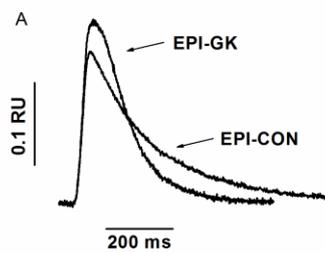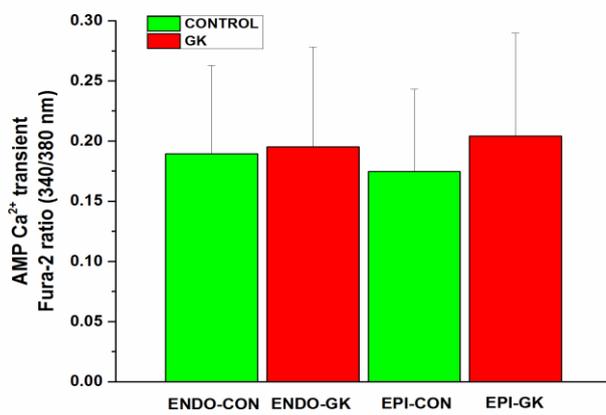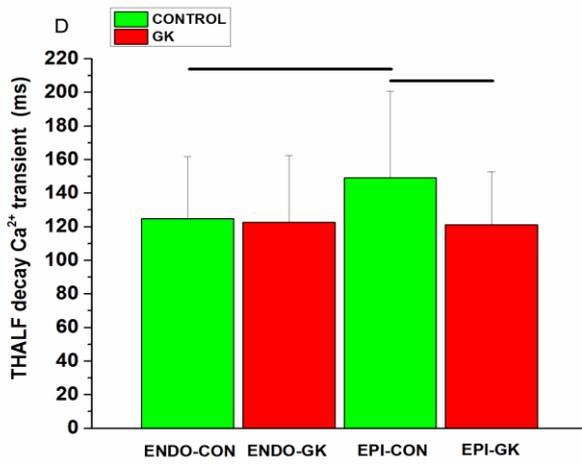
Figure 5 – Sarcoplasmic reticulum Ca^{2+}

Typical record showing protocol employed in a control ventricular myocyte during SR Ca^{2+} experiments (A). Initially Ca^{2+} transients were recorded during electrical stimulation. Electrical stimulation was then paused for 5 sec and 20 mM caffeine was rapidly applied for 10 sec. After application of caffeine, electrical stimulation was resumed. Bar graphs showing mean amplitude of caffeine-evoked Ca^{2+} transients (B), area under the curve of the caffeine-evoked Ca^{2+} transients (C), fractional release of Ca^{2+} transients (D). Data are mean ± SD, n=22-31 cells from 5-6 GK and CON hearts.
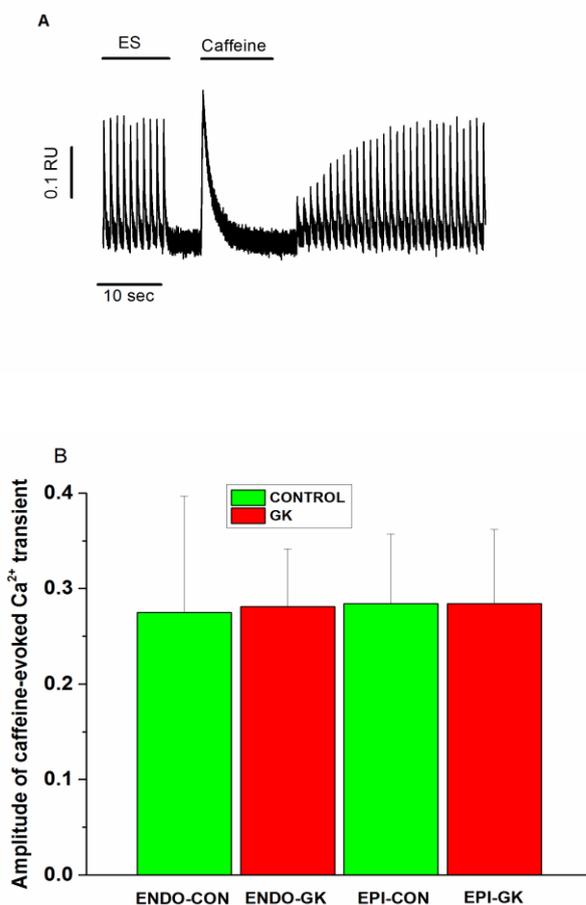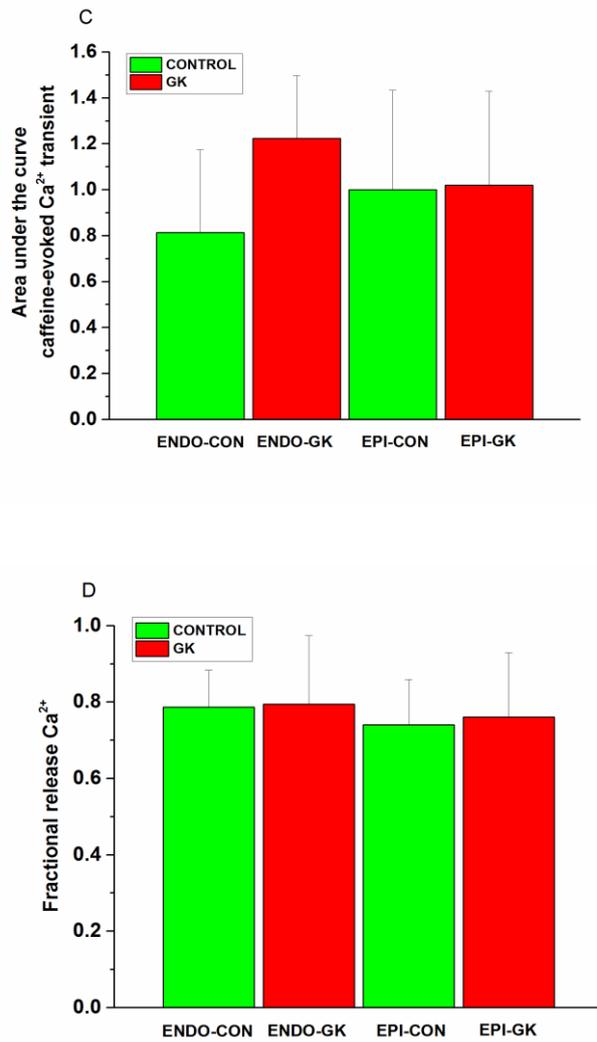
Figure 6 – Ca^{2+} sensitivity of cardiac myofilaments

Typical record of shortening and Ca^{2+} transient (left panel) and a phase-plane diagram of Fura-2 ratio

versus cell length (right panel) in an EPI-CON myocyte are shown in Fig. 6A. Mean gradient of the

Fura-2–cell length trajectory during late relaxation (500-800 ms) of the twitch contraction is shown in

Fig. 6B. Data are mean ± SD, n=18-23 cells from 4-5 GK and CON hearts.